PHYSICAL REVIEW B VOLUME 56, NUMBER 8 15 AUGUST 1997-II

Cyclotron-resonance studies of strongly coupled double quantum wells in tilted magnetic fields near the quantum and semiclassical limits

D. D. Arnone, T. P. Marlow,* and C. L. Foden
Toshiba Cambridge Research Centre Ltd., 260 Cambridge Science Park, Milton Road, Cambridge CB4 4WE, United Kingdom

E. H. Linfield, D. A. Ritchie, and M. Pepper
Cavendish Laboratory, University of Cambridge, Madingley Road, Cambridge CB3 OHE, United Kingdom

(Received 24 March 1997)

Far-infrared cyclotron-resonance (CR) spectroscopy has been used to study a pair of strongly coupled two-dimensional electron gases (2DEG's) which were formed in two GaAs quantum wells and separated by a thin $Al_xGa_{1-x}As$ barrier. The degree of wave-function hybridization, along with the effect of a magnetic field parallel to the plane of the electron gas, have been investigated near both the quantum and semiclassical limits, corresponding to low and high filling factors, respectively. Near the quantum regime, the CR transitions in the presence of a small parallel field reveal anticrossing between the Landau levels associated with different hybridized subbands. The energies and intensities of these transitions change with front gate bias, yielding information on the bias dependence of the wave-function hybridization and the subband energy splitting. Close to the semiclassical limit and with strong parallel magnetic fields, two CR peaks are observed. The corresponding cyclotron masses are compared to those expected for noncircular Fermi contours created by anticrossing of the parabolic dispersion curves associated with the coupled 2DEG's. Experimental results in both limits are discussed in the light of predictions from self-consistent solutions of Poisson's and Schroedinger's equations. [S0163-1829(97)50832-0]

The physics of strongly coupled two-dimensional electron gases (2DEG's) has recently become the focus of great interest, mainly because of the phenomena which arise as a consequence of wave-function hybridization between the adjacent gases. With the application of parallel and perpendicular magnetic fields to such a system, a variety of phenomena not present in single 2DEG's are observed at low and high filling factors ν, corresponding to regions near the quantum and semiclassical limits, respectively. Whilst numerous dc electrical investigations (e.g., Refs. 1 and 2) have been performed on such systems in these limits, very few far-infrared (FIR) cyclotron-resonance (CR) investigations have been undertaken. Here, we reconcile the FIR response in the quantum regime to theoretical models of this system, using gate bias to map out the dependence of the response on wave-function hybridization and subband energy separation. Further, near the semiclassical regime, we see the appearance of a second CR absorption peak at large parallel fields.

The heterostructure used for these investigations was grown by molecular beam epitaxy (MBE) and consisted of two 95 Å modulation-doped GaAs quantum wells separated by a 16 Å $Al_{0.33}Ga_{0.67}As$ barrier. Ohmic contacts to both wells were formed using an annealed $Ni_xAu_{1-x}Ge$ metallization, a 1.8 mm^2 mesa was wet-etched chemically, and 80 Å of NiCr was evaporated as a semitransparent front gate. The total carrier density and the mobility were $N=5.9\times10^{11}$ cm^{-2} and $\mu=630\ 000$ cm^2/Vs, respectively, at $T=3.3$ K.

Figure 1 depicts the carrier densities of the two occupied subbands, N_s and N_a, as a function of front gate bias (V_{fg}), and was derived from Shubnikov de Haas (SdH) data. Note that the experimental data implies the device is electrically asymmetric as might be expected due to dopant diffusion during growth of the layers. Also shown for comparison are the densities predicted by the numerical simulation based on self-consistent solutions of Poisson's and Schroedinger's equations. In the simulation, the effective mass was taken to be constant in the wells, and the rectangular barriers were assumed to be perfect and of constant thickness. Despite these limitations, Fig. 1 shows good agreement between experiment and simulation over most of the front gate bias range if asymmetric doping is also used in the model. The predicted subband separation is also plotted in Fig. 1 and it can be seen that the two wells were on resonance, corresponding to minimum subband separation, when $V_{fg}=$

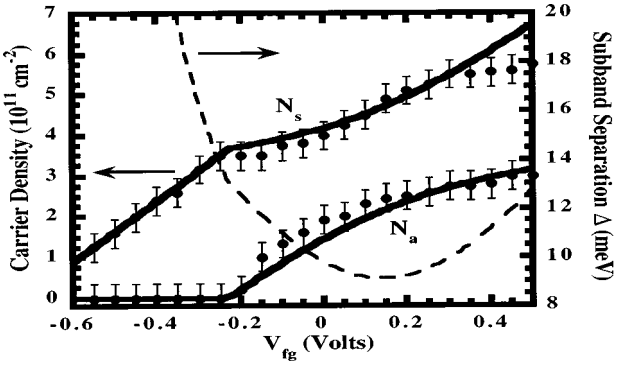

FIG. 1. Carrier densities of subbands corresponding to symmetric (N_s) and antisymmetric (N_a) states as a function of front gate bias V_{fg}. Solid circles are experimental densities extracted from dc magnetoresistance measurements at $T=3.3$ K, and solid lines are densities derived from the numerical simulation. The dashed line represents the energy separation Δ between these states calculated from the simulation.

$+0.14$ V. This point of complete wave-function hybridization was close to the value of $V_{fg}=+0.09(\pm 0.04)$ V estimated from the minimum separation between N_s and N_a in Fig. 1, confirming the different numbers of ionized dopants in each layer. Significant wave-function hybridization was predicted between the strongly coupled wells over the entire range of V_{fg}, even away from the resonance bias. The simulation suggested that the lower energy subband at $B=0$ T (N_s) was predominantly symmetric across the entire double-well region, whereas the higher energy subband (N_a) was mainly antisymmetric [see inset of Fig. 3(a)].

The FIR response of such a strongly coupled structure was investigated in the presence of parallel ($B_\parallel$) and perpendicular ($B_\perp$) magnetic fields, with CR spectra recorded at combinations of V_{fg}, $B_\parallel$, and $B_\perp$ with $T=3.3$ K. Transmission spectra $T(V_{fg},B_\parallel,B_\perp)$ were normalized with a reference spectrum $T_{ref}(V_{fg}=-0.86V,B_\parallel,B_\perp)$ where both wells were totally depleted of electrons. Results were plotted as the relative transmission $-\Delta T/T_{ref}=(T_{ref}-T)/T_{ref}$. Unpolarized radiation was used at near-normal incidence, and $B_\parallel>0$ T was achieved by tilting the normal to the plane of the gases at an angle θ to the applied field, so that $\tan\theta=B_\parallel/B_\perp$. Two regimes were investigated, corresponding to low and high filling factors $\nu_i=hN_i/eB_\perp$, where the subband index $i=a,s$ refers to the antisymmetric and symmetric subbands, respectively. The region near the quantum limit was explored using $B_\perp\leqslant 7.73$ T, $B_\parallel\leqslant 2.73$ T, and $V_{fg}\leqslant -0.10$ V, giving values of $\nu_s\leqslant 3$ and $\nu_a\leqslant 2$. Closer to the semiclassical limit, the effects of high parallel fields $B_\parallel\approx 7$ T were studied for weaker $B_\perp\sim 2.4$ T and $V_{fg}=+0.50$ V, yielding $\nu_s=11$ and $\nu_a=8$. In both limits, CR spectra with $B_\parallel\neq 0$ T were compared to those with $B_\parallel=0$ T.

The motivation for applying a parallel field near the quantum limit is to couple electron motion in the confinement direction (z) to cyclotron motion in the plane of the wells. Without such $B_\parallel$-induced coupling, normally incident FIR radiation excites transitions between Landau levels in the same subband only. The coupling relaxes the selection rules and enables such radiation to excite transitions between different Landau levels associated with each of the electric subbands, resulting in a splitting of the single CR peak at $B_\parallel=0$ T into two when $B_\parallel\neq 0$ T.[3] These new transitions are strongest when $\Delta=\hbar\omega_{ac}$, where Δ refers to the subband separation in the wells and $\hbar\omega_{ac}$ is the cyclotron energy at the anticrossing field $B_\perp=B_{ac}$ where the coupling is greatest. The observation of the CR splitting thus provides a convenient means for estimating Δ. This $B_\parallel$-induced mixing of Landau levels and electric subbands can be seen explicitly in the Hamiltonian

$$H=\frac{p_X^2}{2m^*}+\tfrac{1}{2}m^*\omega_C^2X^2+\frac{p_z^2}{2m^*}+V(z)+\frac{e^2B_\parallel^2z^2}{2m^*}+\frac{e^2B_\perp B_\parallel Xz}{m^*},\qquad(1)$$

where $X=x+\hbar k_y/eB_\perp$.

$V(z)$ is the potential arising from ionized donors, band-structure discontinuities, and the free charge, and $B_\parallel$ is applied along the y axis in the plane of the 2DEG's. Using this Hamiltonian, the Schroedinger and Poisson equations were solved self-consistently. The last term in Eq. (1) which couples the parallel and perpendicular electron motion was treated using degenerate perturbation theory, which yielded a mixture of Landau levels (eigenstates of the first two terms in the Hamiltonian) and hybridized subbands (eigenstates of the next three terms), producing an anticrossing near $\Delta=\hbar\omega_{ac}$. Along with the strong mixing of the hybridized wave functions, significant splitting of the cyclotron resonance peak was predicted near appropriate values of V_{fg} and $B_\perp$.

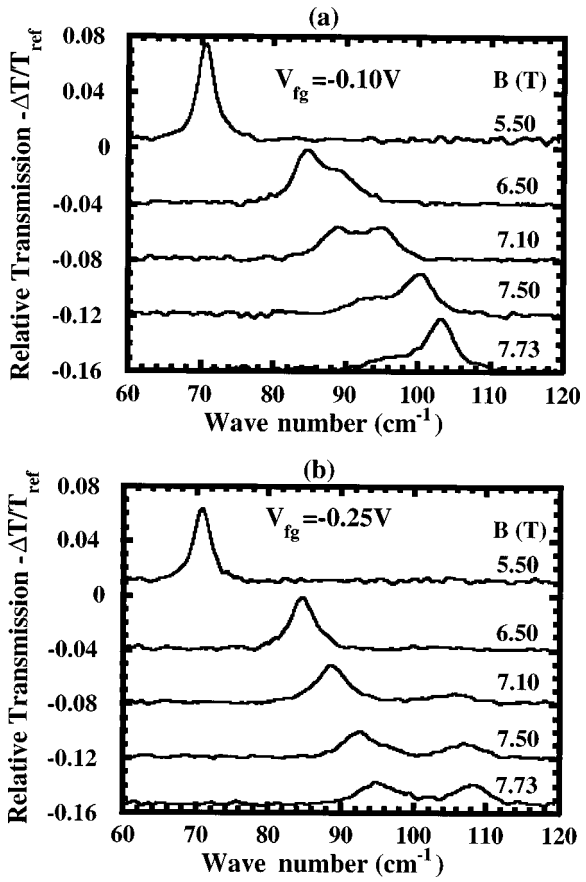

FIG. 2. Relative transmission $-\Delta T/T_{ref}$ as a function of wave number at (a) $V_{fg}=-0.10$ V, and (b) $V_{fg}=-0.25$ V ($T=3.3$ K), for various magnetic fields applied at 15° to the normal of the plane of the coupled wells.

At the anticrossing point (B_{ac}), one would expect to see both a minimum energy separation between the two CR peaks and equal peak intensities. This behavior is clearly seen in Figs. 2(a) and 2(b) which show spectra near the quantum limit at a fixed angle $\theta=15°$ for biases $V_{fg}=-0.10$ V and -0.25 V, respectively. In both cases, the single peak at $B_\perp=5.50$ T was split into two peaks as the field increased towards B_{ac}, commensurate with a leveling of the peak intensities. Note that the probability of a transition between states involved in anticrossing but in different electric subbands reduces for fields away from B_{ac}, so two peaks were not observed in these regions. Figures 3(a) and 3(b) show the measured peak positions as a function of $B_\perp$ for the data shown in Fig. 2, along with the relevant positions predicted by the simulation. Good agreement can be seen between theory and experiment. The simulation suggested that for $V_{fg}=-0.25$ V, anticrossing between the first excited Landau

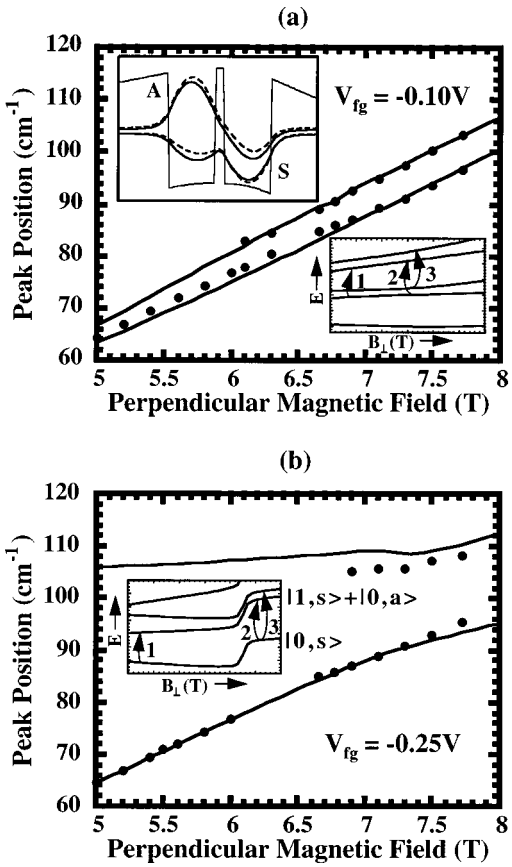

FIG. 3. Spectral peak position as a function of perpendicular magnetic field for (a) $V_{fg}=-0.10$ V and (b) $V_{fg}=-0.25$ V at an angle of 15° ($T=3.3$ K). Circles represent experimental peak positions whilst solid lines are predictions from the model for the transitions shown in the corresponding inset. These insets show calculated energy levels E as a function of $B_\perp$ over the same field range. The large inset in (a) shows the occupied subband wave functions at $B=0$ T as a function of z for $V_{fg}=-0.10$ V (solid lines) and $V_{fg}=-0.25$ V (dotted lines).

level of the lower energy symmetric state $|1,s\rangle$ and the ground Landau level of the higher energy antisymmetric state $|0,a\rangle$ would occur at $B_\perp=8.10$ T. This field is close to the value of $B_{ac}=7.73$ T determined experimentally from the observations of equal peak intensities and minimum energy separation. The inset of Fig. 3(b) shows the transitions between these calculated energy levels (labeled 2 and 3) together with the single $|0,s\rangle$ to $|1,s\rangle$ transition seen at low $B_\perp$ (labeled 1). The shift of intensity between the CR peaks as $B_\perp$ was swept through B_{ac} was also in good quantitative agreement with the simulation and reflected the variation in wave-function mixing around B_{ac}. At $V_{fg}=-0.10$ V, similar behavior was seen, but a lower value of B_{ac} and higher Fermi energy resulted in a more complicated transition structure. Below $B_\perp\sim 6.7$ T the $|1,s\rangle$ to $|2,s\rangle$ transition [labeled 1 in the inset of Fig. 3(a)] was dominant in the spectrum. At $B_\perp\gtrsim 6.7$ T, comparison with theory suggested that transitions were occurring from two initial levels comprised of different mixtures of the $|1,s\rangle$ and $|0,a\rangle$ states to two final levels containing different combinations of the $|2,s\rangle$ and $|1,a\rangle$ states. These transitions are labeled 2 and 3 in the inset of Fig. 3(a), showing the initial and final states.

Comparisons between the experimental and simulation data in the quantum limit have explicitly demonstrated the hybridized nature of the subbands in the strongly coupled structure. Whilst such an FIR response has been measured before,[4,5] no self-consistent simulations or investigations as a function of gate bias have been performed. We have, however, shown here that the bias, and hence the electric field, play an important role both in determining the subband separations and in forming the hybridized wave functions. Thus, the subband separation in the wells at the resonance bias ($V_{fg}\sim+0.10$ V) was $\Delta=9.1(\pm0.1)$ meV (see Fig. 1). By contrast, at $V_{fg}=-0.25$ V the experimental anticrossing field in Fig. 3 implied an increase in subband separation to $\Delta=13.3(\pm0.3)$ meV. This value is in good agreement with $\Delta=13.5$ meV predicted by the simulation. At $V_{fg}=-0.10$ V, taking $B_{ac}=7.1(\pm0.1)$ T yields the estimate $\Delta=12.2(\pm0.3)$ meV, which is again in reasonable agreement with the data in Fig. 1. This variation in subband separation resulted from an increasing perturbation of the symmetric and antisymmetric states for progressively more negative V_{fg} and is illustrated in the inset of Fig. 3(a). Note, however, that Δ at these biases was still much less than the subband spacing associated with uncoupled wells (~94 meV), implying significant hybridization and, overall, symmetric and antisymmetric wave-function characteristics.

The FIR CR response near the semiclassical limit was investigated by comparing the response at $B_\parallel=0$ T with that at $B_\parallel\neq0$ T for weak perpendicular field values ($B_\perp\leqslant2.74$ T). For suitably large values of $B_\parallel$ applied along the y axis in the plane of the 2DEG's, significant anticrossing between the 2D parabolic dispersion curves associated with the individual electric subbands has been predicted, resulting in the formation of two new curves with energies which are nonparabolic in momentum coordinate k_x.[6] To calculate these curves in the presence of weak $B_\perp$, the semiclassical approximation[7] was used, with the Hamiltonian given by

$$H=\frac{p_y^2}{2m^*}+\frac{p_z^2}{2m^*}+V(z)+\frac{1}{2m^*}(\hbar k_x+eB_\parallel z)^2, \qquad (2)$$

where $B_\perp=0$ T. A self-consistent quantum mechanical calculation was first performed to determine the electric subbands of the coupled system, and the dispersion relation in $B_\parallel$ was then found by evaluating Eq. (2) for each value of k_x. The perpendicular field was finally included using quasiclassical quantization rules, with the energies of the Landau levels being determined by the requirement that each real-space electron trajectory must include an integer number of flux quanta. The two new Fermi contours associated with each of the dispersion curves were characterized by two cyclotron masses.[6] The inset in Fig. 4 shows predictions of the new contours and their cyclotron masses for $B_\parallel=7.61$ T and $B_\perp=2.46$ T. To maintain the validity of the semiclassical approximation and to ensure adequate spectral signal to noise ratio (SNR) at large tilt angles $\theta\geqslant70°$, $V_{fg}=+0.50$ V was used in both simulation and experiment.

Figure 4 presents CR spectra recorded at a variety of tilt angles $\theta\geqslant70°$, yielding spectra at different $B_\perp$ whilst keeping $B_\parallel$ roughly constant. Also shown for comparison are spectra recorded at $\theta=0°$ which have the same $B_\perp$ values but $B_\parallel=0$ T. The main difference is the presence of two peaks at large $B_\parallel$ compared with the single peak at $B_\parallel=0$ T. The

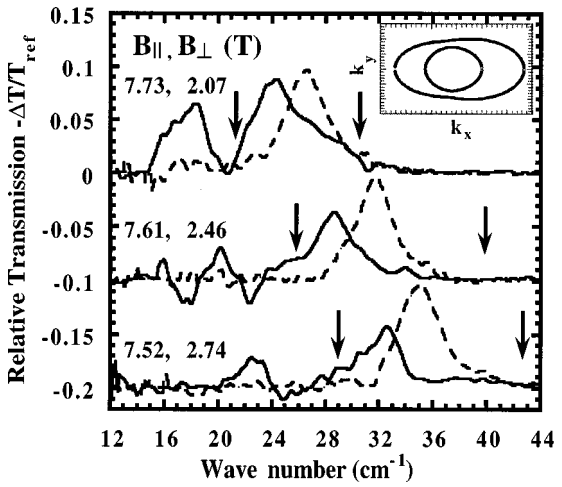

FIG. 4. Relative transmission $-\Delta T/T_{\mathrm{ref}}$ as a function of wave number for $V_{\mathrm{fg}}=+0.50$ V at various magnetic fields ($T=3.3$ K). Solid lines are spectra recorded at the values of $B_{\perp}$ and $B_{\parallel}\neq 0$ T indicated. Dashed lines are spectra recorded at identical $B_{\perp}$ but with $B_{\parallel}=0$ T for comparison. Arrows denote peak positions predicted by numerical simulation. Inset shows Fermi contours for $B_{\parallel}=7.61$ T and $B_{\perp}=2.46$ T; the inner and outer contours have relative cyclotron masses of 0.81 and 1.25, respectively.

experimental configuration also allowed similar $B_{\perp}$ to be investigated at low $B_{\parallel}\sim 0.6$ T ($\theta\sim 15°$), where again only single peaks were observed. The peak positions calculated by the simulation for the given $B_{\perp}$,$B_{\parallel}$ combinations are indicated by the arrows in Fig. 4. Qualitative agreement between the simulation and experimental observations can be seen, allowing the two peaks to be attributed to the formation of two Fermi contours. The simulation also suggested that only single peaks would be distinguished at $\theta\sim 15°$ with positions close to those for $\theta=0°$, again agreeing with the experimental observations.

Whilst the prediction of two Fermi contours was qualitatively supported by the spectra, good quantitative agreement was not achieved. There are two possible sources of error. First, the accuracy of the semiclassical approximation decreases for increasing $B_{\perp}$, implying that the approximation may not be fully justified over the range of $B_{\perp}$ investigated here. In particular, the probability of electron tunneling between the two contours (magnetic breakdown) (Ref. 8) is $\sim 30\%$, implying a more complicated picture than that in the inset of Fig. 4. Second, the small inaccuracies in the simulation at very high bias (see Fig. 1) may become significant.

In conclusion, the FIR magneto-optical response of two strongly coupled electron gases was recorded systematically both in the quantum and near the semiclassical regimes as V_{fg}, $B_{\perp}$, and $B_{\parallel}$ were altered. The CR spectra in the quantum limit revealed $B_{\parallel}$-induced anticrossing between the Landau levels associated with different electric subbands. This allowed the subband separation and wave-function hybridization to be explicitly mapped out as a function of gate bias. Adjusting the bias away from the resonance point increased the subband separation and perturbed the symmetric and antisymmetric wave functions, but did not completely destroy the hybridization. Towards the semiclassical regime, two peaks at high $B_{\parallel}$ and V_{fg} were discovered, in marked contrast to the single peak usually seen in the CR spectra of uncoupled 2DEG's under similar conditions. These peaks were predicted by the numerical simulation and resulted from $B_{\parallel}$-induced anticrossing of the dispersion curves associated with the electric subbands of the coupled system.

*Also at the Cavendish Laboratory.

[1] G. S. Boebinger, H. W. Jiang, L. N. Pfeiffer, and K. W. West, Phys. Rev. Lett. **64**, 1793 (1990).

[2] J. A. Simmons, N. E. Harff, and J. F. Klem, Phys. Rev. B **51**, 11 156 (1995).

[3] A. D. Wieck, F. Thiele, U. Merkt, K. Ploog, G. Weimann, and W. Schlapp, Phys. Rev. B **39**, 3785 (1989).

[4] W. J. Li, B. D. McCombe, J. P. Kaminski, S. J. Allen, M. I. Stockman, L. S. Muratov, L. N. Pandey, T. F. George, and W. J. Schaff, Semicond. Sci. Technol. **9**, 630 (1994).

[5] A. Lorke, U. Merkt, F. Malcher, G. Weimann, and W. Schlapp, Phys. Rev. B **42**, 1321 (1990).

[6] S. K. Lyo, Phys. Rev. B **51**, 11 160 (1995).

[7] L. Smrcka and T. Jungwirth, J. Phys. Condens. Matter **6**, 55 (1994).

[8] J. Hu and A. H. MacDonald, Phys. Rev. B **46**, 12 554 (1992).